BEILSTEIN JOURNAL OF NANOTECHNOLOGY

Supporting Information

for

Electron-induced deposition using $Fe(CO)_4MA$ and $Fe(CO)_5$ – effect of MA ligand and process conditions

Hannah Boeckers, Atul Chaudhary, Petra Martinović, Amy V. Walker, Lisa McElwee-White and Petra Swiderek

Beilstein J. Nanotechnol. **2024,** *15,* 500–516. doi:10.3762/bjnano.15.45

Additional figures and tables

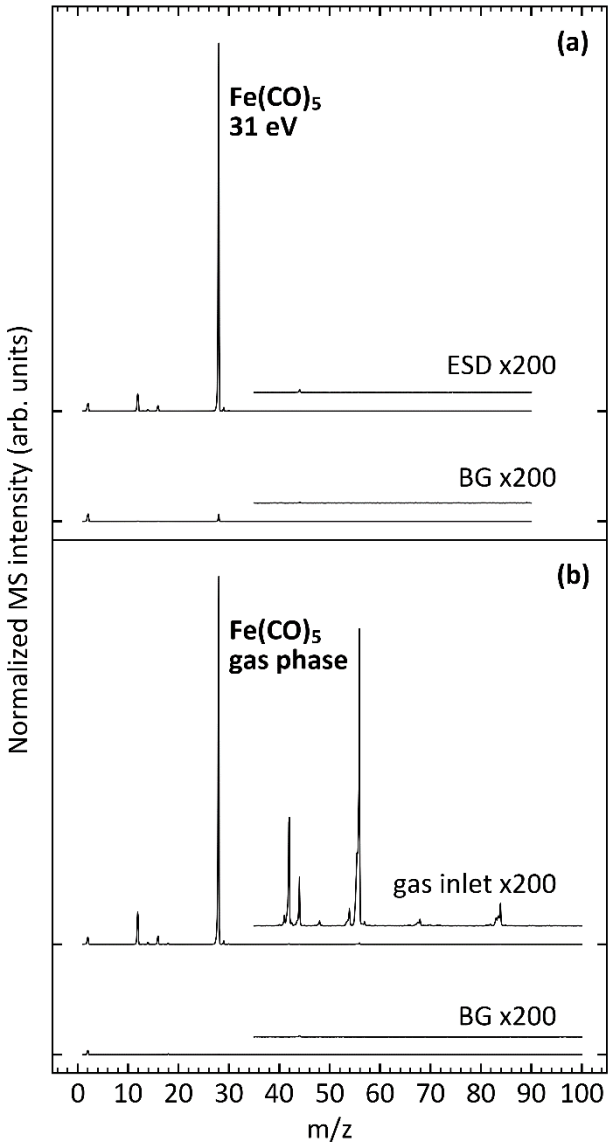

Figure S1: (a) ESD of neutral species during irradiation with 31 eV electrons from an $Fe(CO)_5$ multilayer on a Ta substrate held at 100 K (ESD). The thickness of the condensed layer was roughly 4 monolayers. (b) Mass spectra recorded during leaking of $Fe(CO)_5$ into the UHV chamber (gas inlet). Both data sets include a background mass spectrum (BG) recorded immediately prior to precursor leakage and electron irradiation, respectively. Ticks on the vertical axis indicate the baseline for each curve.

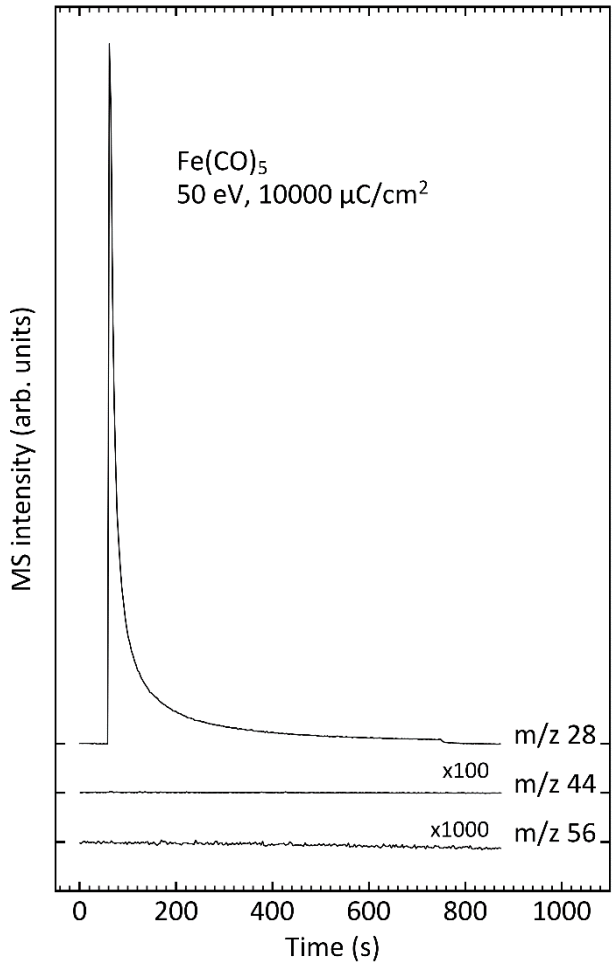

Figure S2: Time evolution of characteristic ESD signals recorded during irradiation with 50 eV electrons from an $Fe(CO)_5$ multilayer on a Ta substrate held at 100 K. The thickness of the condensed layer was roughly 5 monolayers. *m/z* 28 represents desorption of CO, *m/z* 56 was recorded to determine if Fe-containing species desorb. *m/z* 44 was monitored to search for desorption of CO_2. The total electron exposure was 10000 μC/cm^2. Ticks on the vertical axis indicate the baseline for each curve at the beginning of the experiment.

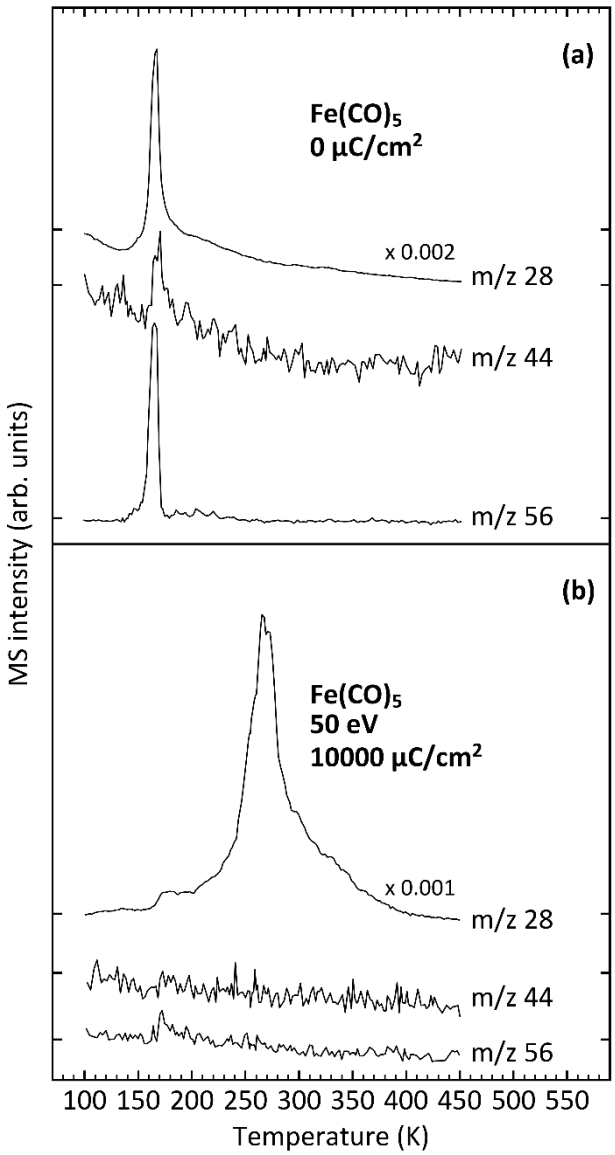

Figure S3: TDS obtained (a) from a pristine $Fe(CO)_5$ multilayer and (b) from an $Fe(CO)_5$ multilayer after irradiation with a total electron exposure of 10000 μC/cm^2 at 50 eV shown in Figure S2. The thickness of the condensed layers prepared on a Ta substrate held at 100 K was roughly 5 monolayers. Ticks on the vertical axis indicate the baseline for each curve at the beginning of the experiment. A slope in the baseline was due to pumping of residual precursor gas from the chamber.

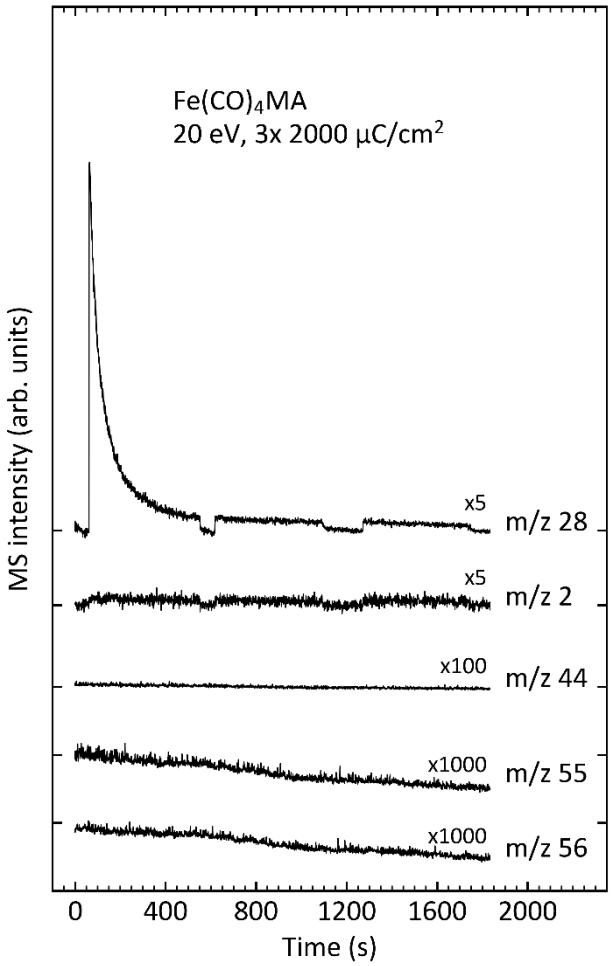

Figure S4: Time evolution of characteristic ESD signals from an $Fe(CO)_4MA$ multilayer on a Ta substrate held at 100 K, recorded during irradiation with 20 eV electrons. The thickness of the condensed layer was roughly 5 monolayers. *m/z* 28 represents desorption of CO, *m/z* 2 is H_2, and *m/z* 55 and 56 were recorded to determine if Fe-containing species or the free ligand or fragments thereof desorb. *m/z* 44 was monitored to search for desorption of CO_2. Irradiation was performed in three steps, each consisting of electron exposures of 2000 $\mu C/cm^2$. Ticks on the vertical axis indicate the baseline for each curve at the beginning of the experiment. A slope in the baseline was due to pumping of residual precursor gas from the chamber.

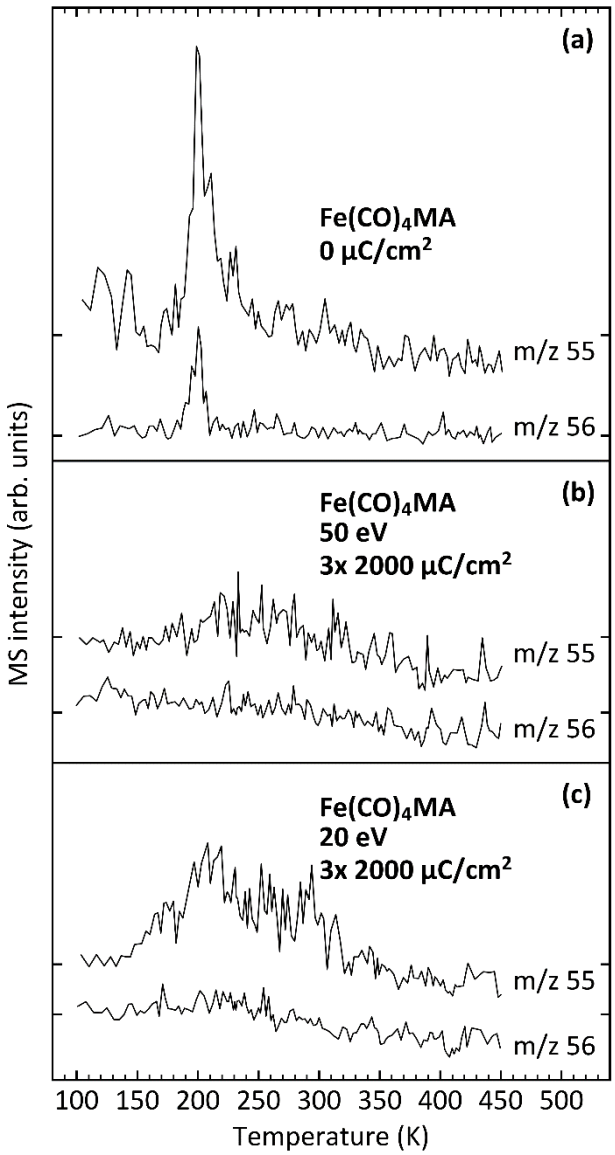

Figure S5: TDS obtained (a) from a pristine $Fe(CO)_4MA$ multilayer without electron irradiation (denoted as 0 $\mu C/cm^2$) and (b) from $Fe(CO)_4MA$ multilayers after three irradiation steps with a total electron exposure of 6000 $\mu C/cm^2$ at 50 eV, and (c) after the same irradiation experiment but performed at 20 eV. The thickness of the condensed layers prepared on a Ta substrate held at 100 K was roughly 5 monolayers. Ticks on the vertical axis indicate the baseline for each curve at the beginning of the experiment. A slope in the baseline was due to pumping of residual precursor gas from the chamber.

Table S1: Summary of deposition experiments by thermal reactions (TDS), room temperature EBID, cryo-EBID, and autocatalytic growth (AG) using $Fe(CO)_5$.

$Fe(CO)_5$	AES PtP heights				Thickness [nm][a]	Fe : C : O (at%)[b]
	Ta	C	O	Fe		
TDS experiments (precursor condensed at 100 K followed by warm-up): Sputtering / AES / 2x TDS (2.5 mTorr) / AES / 2x TDS (2.5 mTorr) / AES						
TDS w/o precursor	62372	4438	6969	0		
	62595	7225	19228	0	0 /0 (1)	0 : 1 : 1.2
	61545	8678	32633	0	0.01/0.01 (2)	0 : 1 : 1.6
TDS 1	55059	9181	11204	0		
	36478	25619	43528	5516	0.16/0.26 (2x)	1 : 8.9 : 6.6
	31384	28628	47306	7702	0.21/0.36 (4x)	1 : 7.2 : 5.1
TDS 2	55874	9978	10426	0		
	38256	27793	44674	5313	0.14/0.24 (2x)	1 : 10.1 : 7.0
	32856	29579	46932	6828	0.20/0.34 (4x)	1 : 8.3 : 5.7
EBID experiment (precursor dosing at room temperature during electron irradiation): Sputtering / AES / EBID (5 mTorr) / AES / EBID (5 mTorr) / AES						
EBID w/o precursor	62396	4049	6098	0		
50 eV	62684	10064	27564	0	0 /0 (1)	0 : 1 : 1.2
	56943	11873	45537	0	0.04/0.06 (2)	0 : 1 : 1.7
EBID 1, 50 eV	57483	8904	15985	0		
	37552	22304	54787	9628	0.16/0.27 (1)	1 : 4.5 : 4.7
	29259	20180	66745	20019	0.26/0.43 (2)	1 : 1.9 : 2.8
EBID 2, 50 eV	57567	8698	13721	0		
	36336	22804	55371	12694	0.17/0.29 (1)	1 : 3.5 : 3.6
	24071	18468	60976	24382	0.33/0.56 (2)	1 : 1.5 : 2.1
Cryo-EBID experiments (precursor condensed at 100 K, then electron irradiation and warm-up): Sputtering / AES / cryo-EBID (5 mTorr) / AES / cryo-EBID (5 mTorr) / AES						
Cryo-EBID 1, 50 eV	57543	7865	10700	0		
	23787	24736	43934	28178	0.34/0.57 (1)	1 : 1.7 : 1.3
	13511	25533	42896	44919	0.55/0.93 (2)	1 : 1.1 : 0.8
Cryo-EBID 2, 50 eV	56061	7609	10971	0		
	23060	23849	41354	28883	0.34/0.57 (1)	1 : 1.6 : 1.2
	13543	23055	42903	45878	0.54/0.91 (2)	1 : 1.0 : 0.8
Autocatalytic growth experiments (EBID seed deposit from $Fe(CO)_5$, then thermal growth): Sputtering / AES / EBID (5 mTorr $Fe(CO)_5$) / AES / AG (5 mTorr) / AES / AG (5 mTorr) / AES						
AG 1	65309	4714	6953	0		
	41283	29583	49171	12860	0.17/0.29 (EBID)	1 : 4.4 : 3.2
	31209	26257	56175	26249	0.28/0.47 (1)	1 : 1.9 : 1.8
	22389	22615	57624	40104	0.41/0.69 (2)	1 : 1.1 : 1.2
AG 2	66904	5003	6877	0		
	38819	27646	50353	13302	0.21/0.35 (EBID)	1 : 4.0 : 3.2
	29736	24833	54703	23929	0.31/0.52 (1)	1 : 2.0 : 1.9
	21583	21907	56148	35208	0.43/0.72 (2)	1 : 1.2 : 1.3

[a] Thickness calculated from the attenuation of the Ta signal. Upper and lower values result from electron attenuation lengths of Ta_{NNN} electrons in Fe (0.38 nm at 183 eV) as well as in C (0.64 nm at 183 eV) [1], respectively.

[b] Composition derived from peak-to-peak heights of the AES signals weighted by tabulated sensitivity factors at 5 keV for the elements Fe (0.9168 at 705 eV), C (0.4763 at 275 eV), and O (1.1012 at 510 eV) [2] assuming a homogeneous distribution of the elements within the deposit.

Table S2: Summary of deposition experiments by thermal reactions (TDS), room temperature EBID, cryo-EBID, and autocatalytic growth (AG) using $Fe(CO)_4MA$.

$Fe(CO)_4MA$	AES PtP heights				Thickness [nm][a]	Fe : C : O (at%)[b]
	Ta	C	O	Fe		
TDS experiments (precursor condensed at 100 K followed by warm-up): Sputtering / AES / 2x TDS (2.5 mTorr) / AES / 2x TDS (2.5 mTorr) / AES						
TDS w/o precursor	62372	4438	6969	0		
	62595	7225	19228	0	0 /0 (1)	0 : 1 : 1.2
	61545	8678	32633	0	0.01/0.01 (2)	0 : 1 : 1.6
TDS 1	57035	7017	12060	0		
	35532	27409	46533	5650	0.18/0.30 (2x)	1 : 9.3 : 6.9
	28704	29780	49356	5998	0.26/0.44 (4x)	1 : 9.5 : 6.9
TDS 2	55494	8934	11226	0		
	33760	28382	41311	5134	0.19/0.32 (2x)	1 : 10.6 : 6.7
	29460	30940	46577	7115	0.24/0.41 (4x)	1 : 8.4 : 5.5
EBID experiment (precursor dosing at room temperature during electron irradiation): Sputtering / AES / EBID (5 mTorr) / AES / EBID (5 mTorr) / AES /						
EBID w/o precursor	62396	4049	6098	0		
50 eV	62684	10064	27564	0	0.00/0.00 (1)	0 : 1 : 1.2
	56943	11873	45537	0	0.04/0.06 (2)	0 : 1 : 1.7
EBID 1, 50 eV	57299	15401	21606	0		
	32783	28900	57368	11517	0.21/0.36 (1)	1 : 4.7 : 3.7
	18405	29867	65725	23188	0.43/0.73 (2)	1 : 2.5 : 2.4
EBID 2, 50 eV	57543	9569	16819	0		
	30679	29458	53790	12021	0.24/0.40 (1)	1 : 4.8 : 4.1
	15802	29511	68985	24785	0.49/0.83 (2)	1 : 2.3 : 2.3
EBID 1, 100 eV	59037	6984	13706	0		
	26394	30956	51263	15949	0.31/0.51 (1)	1 : 3.7 : 2.7
	12250	31999	51421	34499	0.60/1.00 (2)	1 : 1.8 : 1.2
EBID 2, 100 eV	53708	7202	8644	0		
	23174	30853	43860	18021	0.32/0.54 (1)	1 : 3.3 : 2.0
	12211	30763	42828	31398	0.56/0.95 (2)	1 : 1.9 : 1.1
Cryo-EBID experiments (precursor condensed at 100 K, then electron irradiation and warm-up): Sputtering / AES / cryo-EBID (5 mTorr) / AES / cryo-EBID (5 mTorr) / AES						
Cryo-EBID 1, 50 eV	55504	6975	10461	0		
	8266	27479	45190	19930	0.72/1.22 (1)	1 : 2.7 : 1.9
	2697	28042	44556	23647	1.15/1.94 (2)	1 : 2.3 : 1.6
Cryo-EBID 2, 50 eV	54222	6949	9343	0		
	6792	27112	43469	19126	0.79/1.33 (1)	1 : 2.7 : 1.9
	2827	29151	46850	24854	1.12/1.90 (2)	1 : 2.3 : 1.6
Autocatalytic growth experiments (EBID seed deposit from $Fe(CO)_5$, then thermal growth): Sputtering / AES / EBID (5 mTorr $Fe(CO)_5$) / AES / AG (5 mTorr) / AES / AG (5 mTorr) / AES						
AG 1	55154	5525	8412	0		
	34316	24225	45809	11581	0.18/0.30 (EBID)	1 : 4.0 : 3.3
	27555	26168	48466	13479	0.26/0.44 (1)	1 : 3.7 : 3.0
	23593	28045	52627	15689	0.32/0.54 (2)	1 : 1.8 : 2.8
AG 2	55527	5486	6489	0		
	34241	24407	44110	11555	0.18/0.31 (EBID)	1 : 4.0 : 3.2
	33530	34105	57444	17238	0.19/0.32 (1)	1 : 3.8 : 2.8
	27608	34600	58881	20967	0.27/0.45 (2)	1 : 1.7 : 2.8

[a] Thickness calculated from the attenuation of the Ta signal. Upper and lower values result from electron attenuation lengths of Ta_{NNN} electrons in Fe (0.38 nm at 183 eV) as well as in C (0.64 nm at 183 eV) [1], respectively.
[b] Composition derived from peak-to-peak heights of the AES signals weighted by tabulated sensitivity factors at 5 keV for the elements Fe (0.9168 at 705 eV), C (0.4763 at 275 eV), and O (1.1012 at 510 eV) [2] assuming a homogeneous distribution of the elements within the deposit.

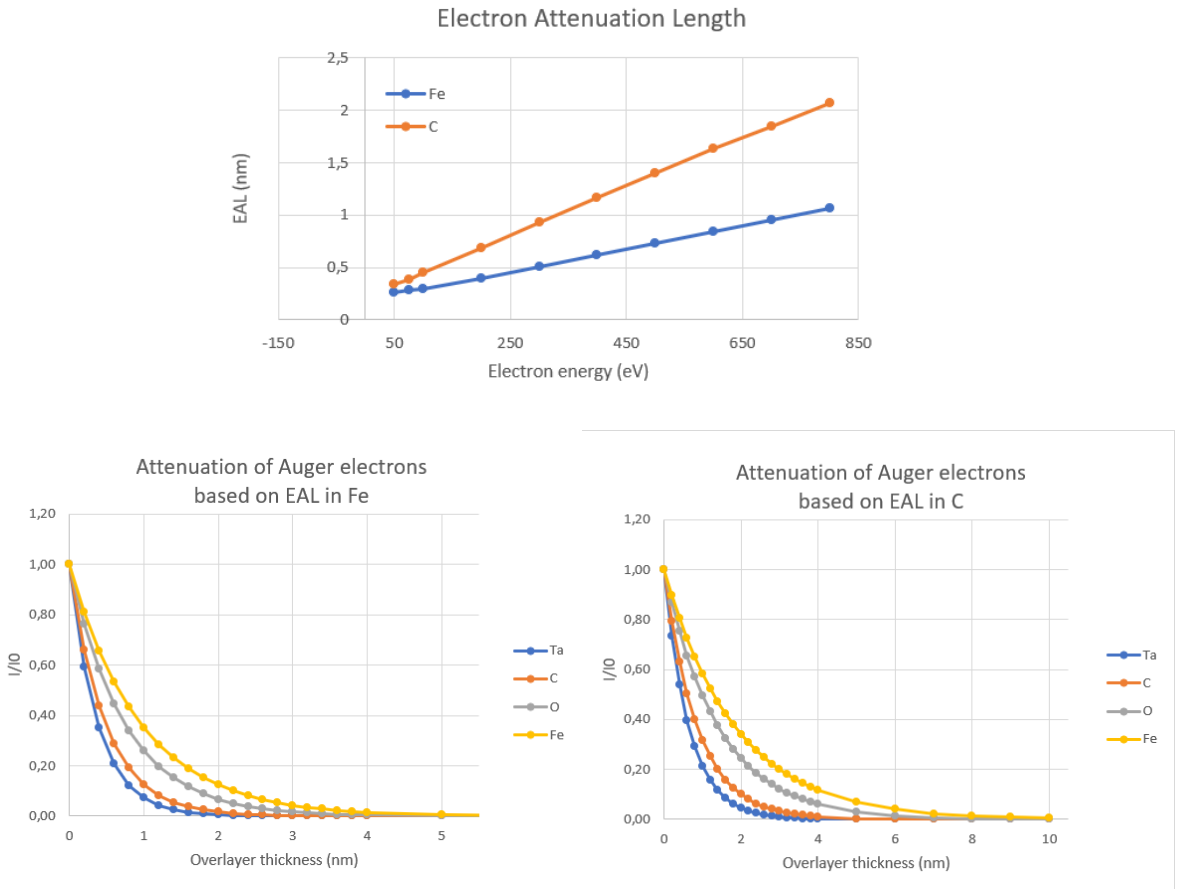

Figure S6: (Top) Electron attenuation length as function of electron energy in pure Fe and C, respectively [1]. These values are used to obtain a lower and upper limit of the deposit thickness from the attenuation of the Ta_{NNN} AES signal as summarized in Tables S1 and S2. (Bottom) Attenuation of Ta_{NNN}, C_{KLL}, O_{KLL}, and Fe_{LMM} AES signal intensities originating from below an overlayer with varying thickness and consisting of pure Fe (left) and C (right), respectively. The intensities were obtained as $I = I_0 \cdot e^{-d/EAL}$ with overlayer thickness d and electron attenuation length EAL for Fe and C, respectively.

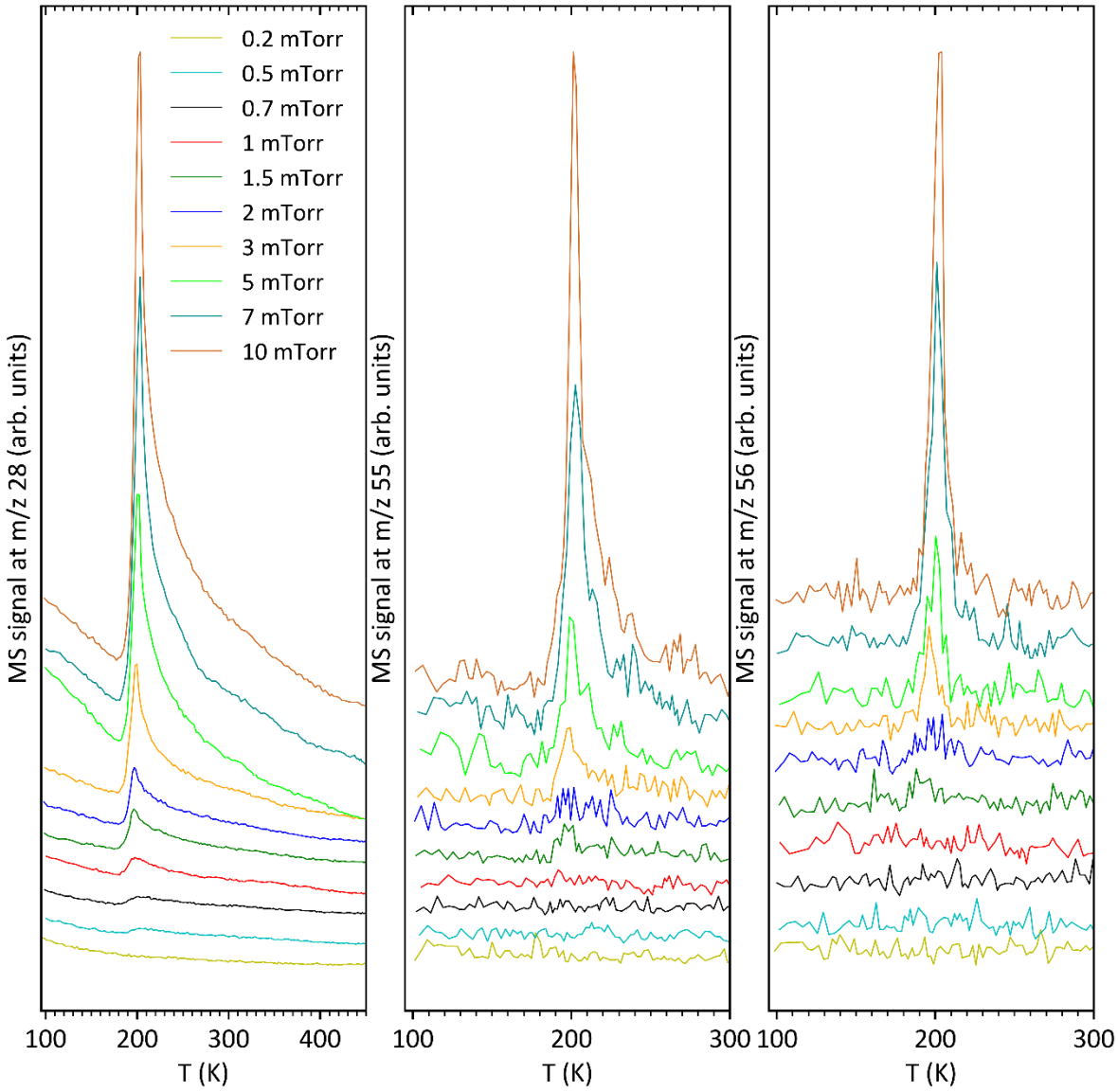

Figure S7: TDS curves obtained for *m/z* 28 (left), *m/z* 55 (middle), and *m/z* 56 (right) after leaking varying amounts of $Fe(CO)_4MA$ onto the Ta substrate. The gas dose is defined as the pressure drop in the gas handing manifold in units of mTorr. A desorption signal in the *m/z* 28 TDS curves ($CO^{\bullet+}$) already appears well below a gas dose of 1 mTorr and develops into a sharp peak near 200 K above that dose. In contrast, signals in the *m/z* 55 and 56 curves ($CH_2CHCO^{\bullet+}$, the dominant fragment of MA, and Fe^+, respectively), indicative of desorption of $Fe(CO)_4MA$, start to emerge only above 1 mTorr. The slope of the baseline that is most noticeable in the *m/z* 28 TDS curves is due to pumping of residual gas in the UHV chamber after leaking of the precursor.

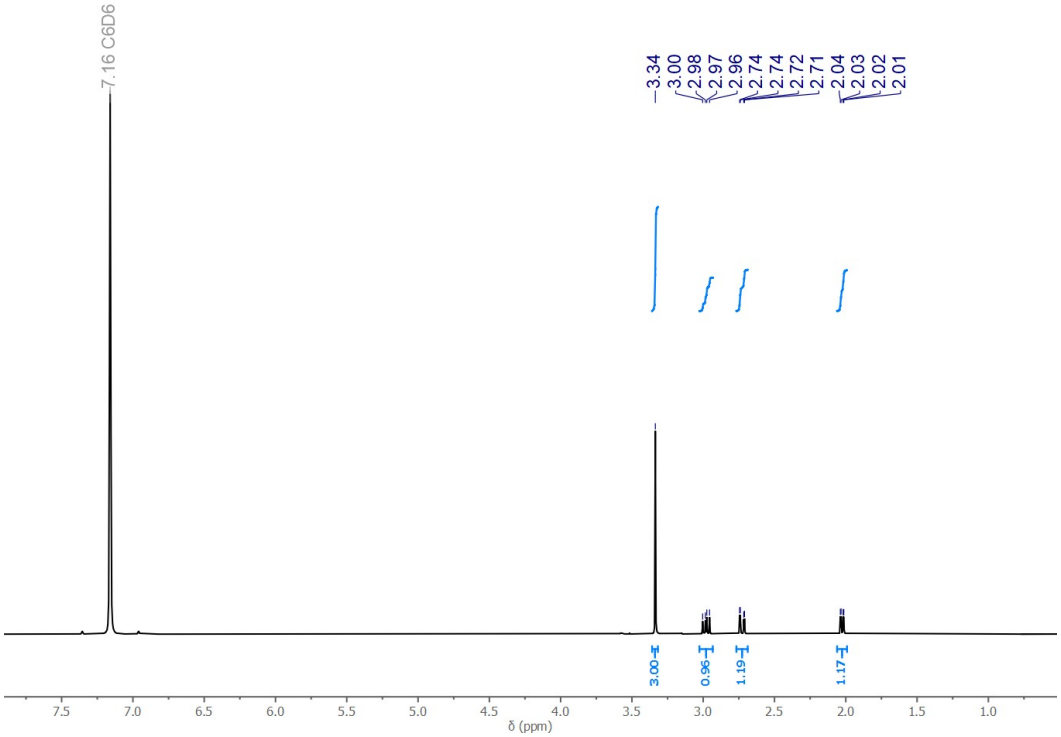

Figure S8: ^{1}H NMR (400 MHz, 25 °C, C_6D_6) spectrum of $Fe(CO)_4MA$ (MA = methyl acrylate, H_2C=CH-$COOCH_3$): δ 3.34 (s, 3H), 2.98 (dd, J = 11.6, 7.8 Hz, 1H), 2.73 (dd, J = 11.6, 2.3 Hz, 1H), 2.03 (dd, J = 7.7, 2.3 Hz, 1H).

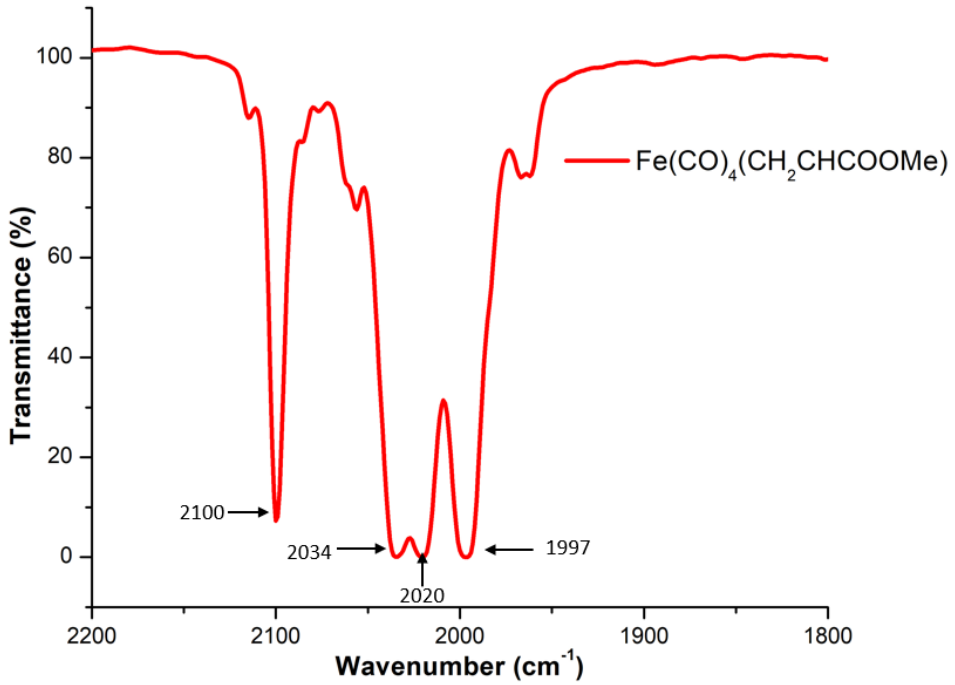

Figure S9: FT-IR spectrum of $Fe(CO)_4MA$ (MA = methyl acrylate, H_2C=CH-$COOCH_3$) obtained in hexane solution: ν_{CO} (cm^{-1}): 2100, 2034, 2020, 1997.

References

[1] P. J. Cumpson and M. P. Seah, Surf. Interface Anal. **25,** 430 (1997).

[2] D. Briggs and J. T. Grant (eds), Surface analysis by Auger and X-ray photoelectron spectroscopy (IM Publications, Chichester, UK and Surface Spectra, Manchester, UK, 2003).